Interplanetary Magnetic Field Measurements at the Magnetopause: Using a Fluxgate Magnetometer on board a Highly-Elliptical Inclined Semi-Synchronous Orbit Satellite

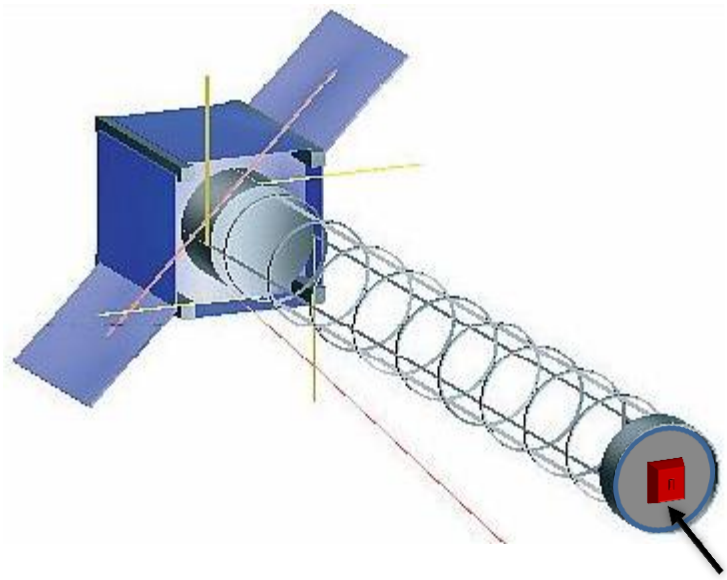

SALMAN H. NAQVI
2nd Year MS/PhD Electrical Engineering, Stanford University
AA 251: INTRO TO SPACE ENVIRONMENT
Prof. Sigrid Close
June 10th, 2012
In partial fulfillment of the class requirements

Index

1. Introduction

In this report, we design a spacecraft that will be used to take interplanetary magnetic field measurements in the magnetopause boundary region by launching it in a highly elliptic orbit and employing a state-of-the-art sensitive fluxgate magnetometer on board. Interplanetary magnetic field (IMF)/ Sun's magnetic field's orientation determines the time and kind of the magnetic reconnection with the terrestrial magnetic field. Thus IMF readings in conjunction with the data from various other scientific instruments can help answer many scientific questions. We outline a few of these questions in the scientific objectives section as a motivation for this project. Then, we start detailing the design of the satellite mission, beginning with launch specifications. The different phases of our mission are then discussed, followed by a discussion about the satellite's orbital mechanics. The focus of the paper, however, remains the scientific measurements part of the mission. Hence, a major part of the effort is devoted to fully explaining the operation of our primary scientific instrument, the fluxgate magnetometer. Its operation, manufacturing, calibration, characteristics, design and performance characteristics are discussed in detail. It is also important alongside to have a clear idea of the data measurements and the anticipated scientific results from the mission. So we have provided an overview of the kind of plots we would expect to analyze under different solar conditions if the mission were to be deemed successful. Finally, we will not be doing justice to the spacecraft design, if we do not fully assess the risk posed by the space environment to the spacecraft as it travels from the mud to the magnetosphere. Hence, in the conclusion to this report, we categorize, in somewhat detail, various hazards posed to the spacecraft and their mitigation techniques. Appropriately accounting for these mitigation techniques and designing, launching, and operating one's spacecraft around these challenges is critical for mission success.

2. Scientific Mission Overview

Scientific Objectives Overview:

The primary scientific objective addressed in this report will be to acquire Interplanetary Magnetic Field (IMF) data in the outer dayside magnetosphere. This scientific objective is a part of a greater mission that combines simultaneously acquired data from multiple scientific instruments on board our satellite to answer broader questions about the magnetospheric dynamics in connection to the solar wind. Some of the broader questions being answered by the satellite mission can be tabulated as follows:

- Determine how the magnetopause responds to solar wind changes
- Furthermore, investigate the internal magnetospheric response of the outer-boundary dynamics

This report will serve to partially answer the first question by acquiring data on the solar wind conditions, i.e. the data on the IMF frozen-in to the solar wind. To get a complete picture of the solar wind at the outer magnetosphere boundary, we would need to acquire the solar wind speed and particle densities. These 3 parameters can be acquired using the Ion Electron Spectrometer (IES) on board our satellite.

IES would make direct measurements of the solar wind ion and electron flux versus incident angle and time. By performing the moment calculations of the ion and electron 3D distribution functions, we can get the solar wind plasma flow speed, and ion and electron densities, all as a function of time. This information would give improved information about the solar wind. This can further allow us to calculate the solar wind dynamic pressure, p_{sw}. When combining this with the magnetic pressure, $p_m = B^2/2\mu_o$, as acquired from the IMF measurements, we can find a key solar wind parameter, solar wind plasma beta, $\beta = p_{sw}/p_m$, which gives us the information about the . However, the operation and implementation of IES and other instruments are beyond the scope of this report.

Specific Scientific Problem:

It is noteworthy to highlight one of the more specific scientific objectives that can be addressed using the IMF data in conjunction with other scientific instruments. This objective is an offshoot of the 1st broader scientific question outlined in the previous section.

> *How are the reconnection and the magnetopause erosion / magnetic flux transfer into the magnetosphere dependent on the IMF orientation, plasma beta and other factors?*
>
> Mass and energy is transferred to the magnetosphere upon the reconnection of the IMF and magnetospheric magnetic fields Fuselier et al. 2007, 2010a and Mozer et al. 2007 have made local measurements of reconnection rate. But in the absence of global observations of magnetopause erosion, global rates of magnetic flux transfer across the dayside magnetopause, which are important for overall magnetosphere energy budget, have not been

measured. We need to know how the magnetic transfer occurs and how is it dependent on IMF orientation and other factors (Petrinec and Fuselier, 2003).

We can make headway in answering this question by making IMF measurements along with simultaneous measurements of solar wind pressure, magnetopause boundary, and the plasmasphere. The magnetopause compression is indicated by an inward magnetopause motion, increase in the solar wind pressure, and high-L brightening of plasmasphere. Thus we would need three more sensors on board the satellite, including a Soft X-ray imager (SXR) for capturing the magnetosphere boundary, IES as described before for solar wind pressure, and the Extreme Ultra Violet (EUV) imager to image the plasmasphere. Afterwards, magnetosphere erosion manifests itself as a southward shift in IMF B_Z, and the equatorward motion of the dayside cusp, captured by the Far Ultra Violet Spectroscopic Imager (FUV) (see figure 2.1). With this study we should be able to monitor the magnetopause for the 30-min erosion event and explore different scenarios of how reconnection and magnetopause erosion depend upon various combinations of solar wind and IMF conditions (Trattner et al, 2007).

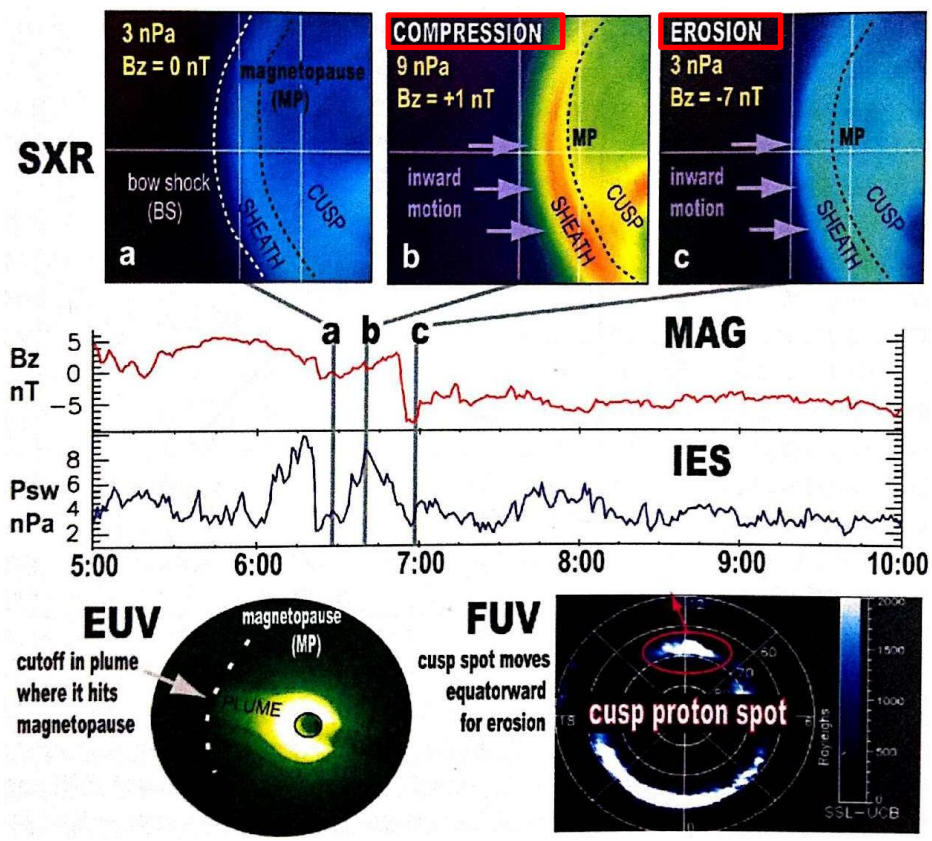

Figure 2.1 – Combining the data from multiple instruments on board the satellite to answer a critical scientific question regarding the magnetic reconnection and magnetopause erosion; solar wind pressure increase is indicated by a point b, while c indicates a southward turning of IMF, indicating magnetic reconnection [Goldstein]

3. Launch Specifications

Launch Location:

We will launch our spacecraft carrying the satellite from the Kennedy Space Center, since this station is the closest one to the equator on the nation's soil (selecting U.S. launch site for better logistical support and long launch heritage). Launching closer to equator gives an extra push to the launch vehicle because a spot at the equator is travelling multifold faster than that at the poles because of the Earth's rotation.

Launch Date and Time:

Launch date and time will be carefully selected after taking into account the data from various useful indexes. Solar activity influences the amount of drag experienced by the launch vehicle in its pursuit to exit the Earth's atmosphere. This is because the enhanced solar flux heats up the atmosphere, which expands; the neutral density at higher altitudes increases. F10.7 cm index is a good measure of the solar flux and a launch date and time will be decided when this index is at low.

Moreover, dry adiabatic lapse rate should also be looked at when selecting the launch time. We should launch in dry conditions when the water vapor content is lower. Otherwise, the troposphere (below 12km) will not be stable to convection and our launch vehicle would experience enhanced turbulence.

It is also desirable to launch the satellite during the solar minimum in order to be able to avoid adverse effects caused by the energetic solar particles on our satellite. Geomagnetic activity results in an enhanced electron precipitation in the auroral regions and the South Atlantic and South East Asian anomalies also get intensified. This increases the probability of SEUs occurrence and ionization damage on board the satellite and the satellite's ground to station communication also gets interrupted as the ionospheric plasma density varies drastically, causing fluctuations in the frequency cutoffs.

However, due to the nature of our mission to measure the IMF during the solar maximum, we will set the tentative launch date of the satellite around 2021 when the sun starts to become active in the solar cycle 25. Furthermore, we will use the Kp and Dst index to estimate the short term solar activity trend, in order to choose a relatively quiescent week for the launch.

4. Orbital Mechanics

Keplerian Orbital Element set:

These have been tabulated below to give a quantitative overview of the location of our orbit [William, 2011]:

Orbital Element	Description	Value
e	Eccentricity – Ratio of Semi-major to Semi-minor axes	.89
a	Semi-major axis	120228km
i	Inclination – Vertical Tilt of ellipse w.r.t. reference (equatorial plane)	61°
Ω	Right Ascension – Longitude of Ascending Node	235°
ω	Argument of Periapsis – Orientation of Ellipse in Orbital Plane	270°
Orbit Period	Days	5
Radius of Perigee	R_E	2
Radius of Apogee	R_E	35

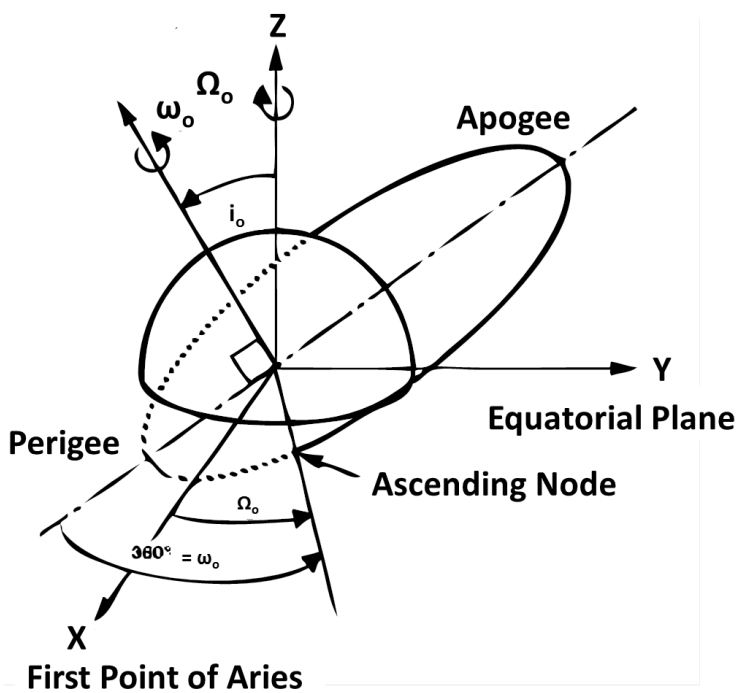

Figure 4.1 – Representation of various Orbital Elements [Johnson, 1992]

Coordinate Sets:

We will make use of a variety of coordinate systems as our spacecraft progresses after launch towards its final destination. Our satellite mission can be divided into multiple phases; starting from the launch location, travelling through the Earth's atmosphere, maneuvering towards the orbit, stationing the spacecraft on orbit, making IMF measurements in the magnetosphere region, to transmitting these measurements to the ground station. Table below lists various coordinate systems appropriate for each mission phase (Bhavnan, 1991, explains these coordinate systems).

Sr. #	Mission Phases	Coordinate Systems
1.	From launch to moving towards the orbit (This coordinate system relates systems of rotating Earth to Inertial/ Quasi-Inertial systems)	*Earth-Fixed Coordinate System* Geocentric (GEOC)/ Geodedic (GEOD)/ Geographic(GEOG)
2.	Stationing the Satellite on Orbit	
	➢ Convert orbital orientation to fixed Earth rotation	*Orbiter Coord. Sys.* Local Orbital (LO) / Local Vertical Local Horizontal (LVLH)
	➢ Display satellite trajectories	Quasi-Inertial Coord. Sys. Geocentric Solar Ecliptic (GSE) / Solar Ecliptic (SE)
3.	Satellite station-keeping and maneuvering on-orbit	
	➢ Satellite Orbit Calculations	*Inertial Coord. Sys.* Aries-True-of-Data (ATD) / Vernal Equinox at Epoch 1950.0 (MS0)
	➢ Satellite Velocity Calculations	ATD (Polar Velocity), M50 (// //) GEOG (// //)
	➢ Space Vehicle Dynamics	Earth Centered Inertial (ECI) Geocentric Celestial // (GCI)
4.	Taking IMF B measurements close to the Earth & near Magnetopause	
	➢ Measurements close to Earth	*Geomagnetic Coord. Sys.* Magnetic, Symmetric Dipole Coord. (MAG)
	➢ Near Magnetopause	Geocentric Solar Magnetospheric (GSM) / Solar Magnetospheric (SMC)
	➢ Analyze components of B	*Local North-East-Vertical Coord. Sys.* Magnetic Field (MFD)
5.	Transmitting data to Ground Stations	
	➢ Defining the position of ground receiving stations	*Earth-fixed / Inertial Coord. Sys.* GEOG/ GEOD/ GEOC

Orbit Type:

We chose our satellite's orbit with the intent of maximizing the viewing time of the magnetosphere by our satellite, so as to study the IMF strength near the magnetospheric boundary / at the reconnection site.

Thus our final destination will be a highly elliptical, high inclination (60°) Earth orbit with the following bounds on the altitude:

Perigee altitude: $2R_E$
Apogee altitude: $35R_E$

Orbital period will be about 5 days, and the spacecraft would spend nearly 4.5 days conducting scientific data acquisition. It shall switch to the standby mode (detailed explanation of the two modes is given in Section 7 under the Magnetometer specifications) as it orbits to within $5R_E$ of the Earth's surface. Our orbit will be near-Molniya orbit (highly elliptic, inclined and semi-synchronous orbit at 64° inclination) ["Army Space Ref"], which will minimize the drift in the location of perigee and hence allowing for the continuation of operation for another year, without requiring orbital maintenance.

Orbital Insertion:

We can achieve our high-apogee orbit using a launch vehicle (LV) and a solid rocket motor (SRM). After the separation from the launch vehicle, SRM initiates a burn to raise the apogee altitude to $35R_E$. At this point, SRM separates from the spacecraft and the spacecraft deploys the solar array (SA).

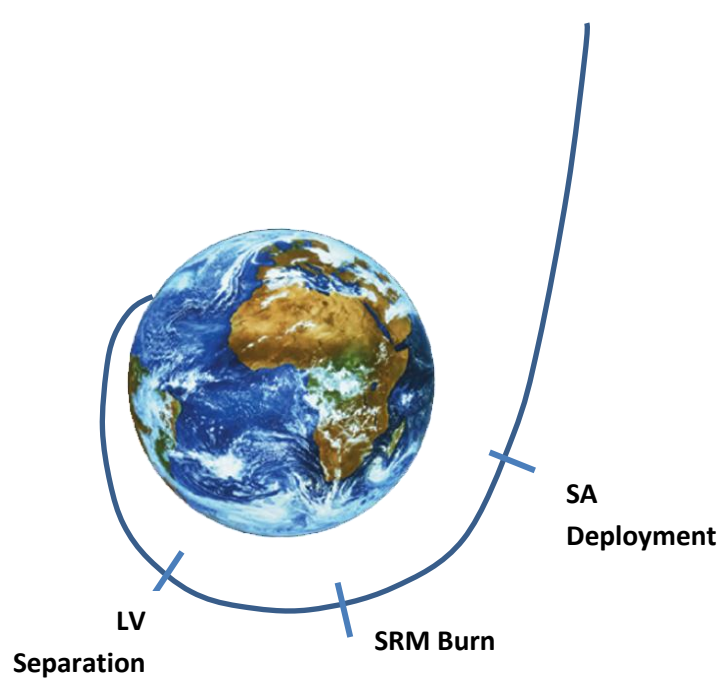

Figure 4.2 – Orbital Insertion Illustration, showing three critical mission events

5. Mission Phases

Mission Milestones:

Our satellite will go through multiple phases, which would be characterized by three critical mission milestones, launch vehicle separation, solid rocket motor firing, and the solar array deployment. Thus following are the key events that lead to the accomplishment of these critical milestones:

1. Spacecraft will be launched some time at the beginning of the next solar cycle, when the sun is beginning to become active. Tentative year of launch is set at 2021, while the exact date will be decided after taking into account the solar flux, adiabatic lapse rate, and weather conditions.
2. Spacecraft would separate from the launch vehicle after it has gained the escape velocity and exits the regions of intense atmospheric drag.
3. Shortly afterwards, SRM would fire the burns to appropriately maneuver the satellite and station it in its high eccentricity orbit with $35R_E$ apogee radius. Such a high apogee would ease synoptic magnetospheric observations, and in-situ investigation of the solar wind.
4. After placing the satellite in orbit, SRM will separate and solar arrays will be deployed. Our spacecraft can then appropriately switch to the science mode and begin collecting data.

Mission Duration and Lifetime:

Spacecraft design lifetime would be about 2 years. During this proposed duration, satellite would take the solar wind B field measurements during the solar maxima. We expect it to give us an indication of IMF and terrestrial field reconnection, by monitoring the switch in the IMF B_Z orientation during the key geomagnetic storms instances. During the solar maximum, we should be able to see more than 20-30 really good storm events for a meaningful reconnection study.

Our orbital design can allow for one or two more years of operation because it is a near-Molniya orbit, demanding little orbital maintenance. However, this decision will be contingent on the propellant budget. During the first two years, spacecraft will pass through the intense radiation environment of the Van Allen belts during its perigee. Thus it should be able to withstand high total ionizing dosage (TID). TID on our satellite is likely to cause some adverse effects on the microelectronics and solar panels. Atmospheric drag will not be an issue for our altitudes. So, depending on the level of ionization damage, we will be able to predict realistic lifetime half a year after the satellite is in orbit.

6. Spacecraft Overview

Scientific Instrument Placement

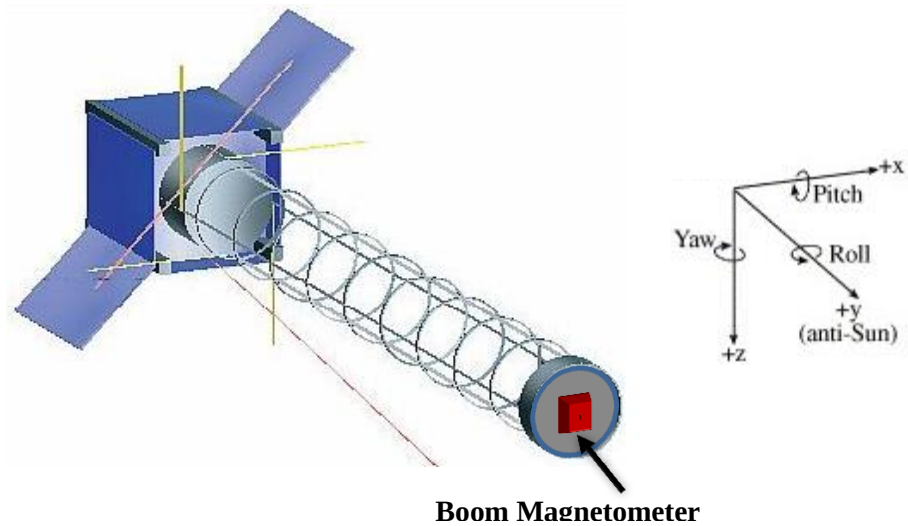

Figure 6.1 – Satellite Schematic with MAG placed on a 3.5m boom [“PRISM”]

MAG sensor will be mounted on a 3.5-meter ATK-Able boom deployed in the –X direction. The boom will receive uniform solar illumination when the satellite is in sunlight. The solar cells will not shadow the boom, thus avoiding the cell-switching transients, and the boom will not be exposed to possible contamination from the thruster fringes.

Satellite Payload Specification

Following table outlines the key features of our satellite payload:

Parameter	Description
Launch Vehicle Compatibility	Taurus 3110 and Athena II
Propulsion	8 monopropellant 4 N thrusters
Attitude Control	3-axis stabilized; 1 ST, 1 IMU, 14 CSS and 3 RW
Momentum Control	Via Thrusters
Deployables	2-panel 2 solar arrays; 3.5 m magnetometer boom
Thermal	Active heater/ passive radiator control
Battery	24 A-hr Li+
Magnetics	<10nT DC and <.1nT AC at the magnetometer
Payload Duty Cycles	100% at > $8R_E$, 83% at <$8R_E$
Commissioning	Instrument turn-on less than 30-days after launch
Telecom	S-band for command, real-time telemetry and ranging, and X-band for stored data/ telemetry

7. Scientific Equipment

Fluxgate Magnetometer

Magnetic field can be measured using various instruments, which include magnetic variometers and magnetometers. There are further classes of magnetometers (MAG), including vapor and liquid MAG and Fluxgate MAG. We will use Fluxgate MAG because it is the simplest and most commonly used for measuring the B field. Moreover, our MAG will have a heritage from the instrument used in many previous missions, including the NASA's GSFC Space Technology 5 (ST5) mission. ST5 fluxgate magnetometer was supplied by UCLA magnetometry group which has supplied MAGs for magnetospheric and solar system magnetic field investigations for over 35 years. Following is the picture of the 3-axis ring core fluxgate sensor fabricated by UCLA.

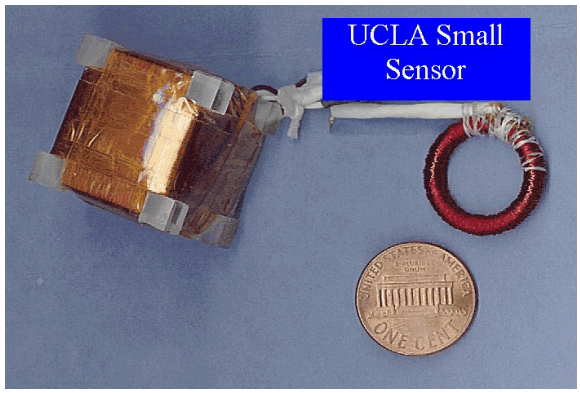

Figure 7.1 – A heritage UCLA ring-core fluxgate magnetometer with a penny in the background [Strangeway, 2001]

MAG operation

A basic circuit diagram describing the working of a fluxgate magnetometer is shown below:

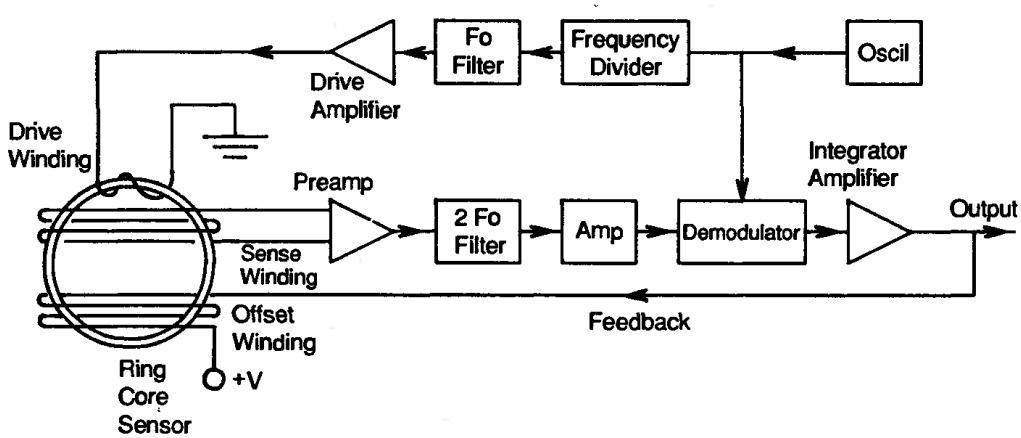

Figure 7.2 - Image Courtesy Kivelson and C.T. Russell, Introduction to Space Physics, Cambridge University Press, 1995

Sensor:

The sensor in the MAG is a transformer with two coils of wire wound around a high-permeability ring core, and hence the name, ring core sensor. High frequency alternating current (5 kHz) excites the transformer's primary winding. The core passes through an alternating cycle of magnetic saturation, i.e. magnetized, demagnetized, inversely magnetized, demagnetized, magnetized and so on. The secondary winding sees an induced time-varying voltage that is related to the input through the core's hysteresis curve.

For high-permeability materials, hysteresis curve is highly non-linear and gives rise to odd harmonics of the drive frequency in the output. In a magnetically neutral background, output will consist of only the odd harmonics, and the input and output would match exactly. When the core is exposed to the magnetic field, it will be more easily saturated in alignment with that field and less easily saturated in opposition to it. This lack of symmetry results in even harmonics as well as the odd ones in the output signal.

However, even harmonics are much weaker than the odd ones, and hence the odd ones, which result from the core hysteresis, must first be eliminated before the weak signals can be detected and amplified. For this, we use ring core transformer with two identical parallel *cores.* Each core is excited by separate coils carrying equal currents in opposite directions. Another secondary coil wound around both the cores will detect a zero output in the absence of an external magnetic field, because the two primary coils will induce exactly equal and opposite effects in the secondary core. And for non-zero magnetic fields, the odd harmonics would still approximately cancel out. The second harmonic is amplified by this process and gives a voltage proportional to the field along the transformer axis.

Figure above shows the schematic for a single sensor. In order to get three components of the vector field, we need three sensors with their transformer axes mutually orthogonal to each other.

Electronics:

A precision oscillator first generates a string of pulses at a frequency twice the final drive frequency of f_o. The signal is passed to the demodulator as a reference, and is then halved and passed through a narrowband filter to the drive amplifier. Now the string of pulses is applied to the primary winding of the transformer. This winding is called the Drive winding. The secondary winding, called the Sense winding, around the transformer detects the total induced voltage and passes it to the pre-amplifier.

Now the signal is again narrow band filtered by twice the drive frequency and further amplified. This amplified output signal is compared by the demodulator against the reference and is made positive or negative based on whether the output leads or lags the reference by 180°. This output which has a frequency twice the drive frequency is integrated and smoothed over many cycles, producing a near-dc voltage.

Final Output:

Amplitude of this near-dc voltage output is proportional to the output of the second harmonic component output by the sensor, and its sign gives the phase of the second harmonic relative to the reference. And these two quantities together are, respectively, proportional to the magnitude and direction of the component of the external magnetic field along the axes of the transformer. This is the low-frequency output of the fluxgate magnetometer.

Null Detection:

Also note here, that through a feedback mechanism this output signal is also used to drive an offset winding around the transformer. This perfectly nulls the magnetic field along the coil's axis, and magnetometer acts as a null detector, making it linear over a large dynamic range.

An elementary explanation is given here in a min. long video by NASA Goddard center, key frames of which have been copied below, where a bar magnet is wrapped around with a coil being supplied with an alternating current, and red arrow indicates an external field. Four key frames from the said video are shown below:

http://www.youtube.com/user/NASAexplorer/videos?query=fluxgate

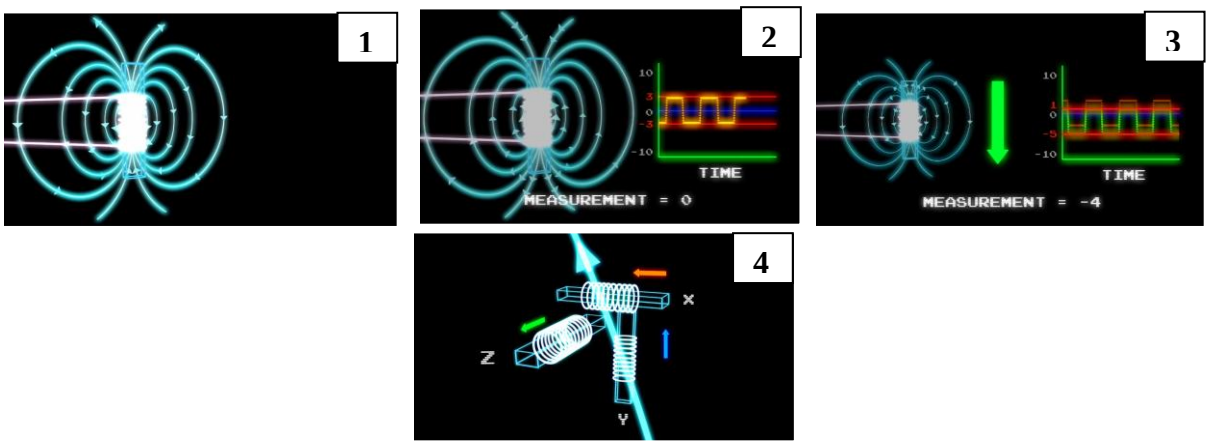

Figure 7.3 – Frames taken from the video developed by NASA GSFC to explain the basic operation of Fluxgate Magnetometers

MAG Specification

Modes:
Our MAG will be able to operate in two modes, a primary "science mode" and a secondary "standby mode." In the first mode, MAG can operate over a dynamic range of ±500nT. MAG will be switched to the "standby mode" when inside the geocentric distances of $5R_E$, where the range will be increased to ±8000nT. In this mode, MAG will stay powered for greater offset stability, and no data transmission will occur except during the commissioning phase.

Performance:
In science mode, MAG will provide B field measurements at up to 2 samples/sec with 16 bit resolution, noise levels less than 10pT/√Hz at 1Hz, and sensitivity as low as 15pT.

Magnetometer Characteristics, Design and Performance Specifications		
Instrument		
Digital Fluxgate Magnetometer		
Characteristics		
Boom Mounted Sensor	Boom length ~ 3.5m	
Electronics in Mission Box	UCLA heritage MAG	
Design Specs		
Mass	Sensor: Cable: Electronics	70g 100g/m +25g / connector 100g
Power	Sensor: Electronics:	75mW 750mW
Data Rate		50 bits / sample
Performance Specs		
Parameter	**Requirement**	**Capability (mode)**
Range	±300nT	±500nT (science) ±8000nT (standby)
Resolution	50pT	15pT (science)
Noise Levels	50pT/√Hz at 1 Hz	20pT/√Hz at 1 Hz (science)
Sample Rate	1 vector /10 sec	2 vector / sec (science)

Table 7.1 – Magnetometer Characteristics, Design, and Performance Specs.

Calibration:
MAG is not an absolute instrument and so needs to be calibrated against standards, so that gains, offsets and sensor orthogonality can be determined. The large non-magnetic test facility at NASA/GSFC with three-axis calibration coils, proton magnetometers and optical theodolites will be used. Additional calibration testing will be conducted on orbit using transverse field fluctuations when the spacecraft is in the solar wind.

Radiation Effects:
MAG sensor is not radiation-sensitive. Moreover, electronics will be radiation hardened. Latch up protection will be provided via over-current limiting resistors.

MAG sensor is, however, immune to various signal interferences. Most notable of which comes from the second harmonic of the drive frequency around 32kHz ± 100Hz. Moreover, transient switching currents from the solar cells can also generate noise. Thus we will establish a cleaning program that identifies such magnetic interference and mitigates it.

Manufactured Unit:
Shown below is the electronic board and chassis of a heritage UCLA magnetometer, which has been radiation hardened:

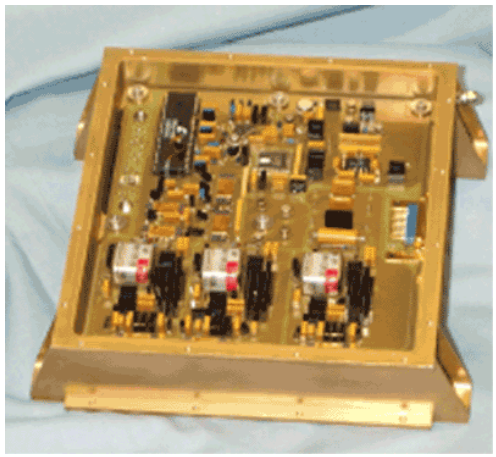

Figure 7.4 – Chassis and Electronic board of a UCLA heritage magnetometer used in the FedSat [Strangeway, 2001]

8. Data Collection & Transmission

Anticipated Measurements

Our MAG will generate level 1 data that consists of the three IMF components in the spacecraft coordinates. These coordinates are transformed into the geophysical coordinates, i.e. GEO, GSM, or SM, using the spacecraft ephemeris. This will be the level 2 data. These data will look like the data displayed in the figure below, Fig. 8.2. It shows the three magnetometer components, which correspond to the IMF Bz, By and Bx using a simple transformation, where F is the total field:

$$X = H\cos(D), \quad Y = H\sin(D).$$
$$F = \sqrt{X^2 + Y^2 + Z^2} = \sqrt{H^2 + Z^2}.$$

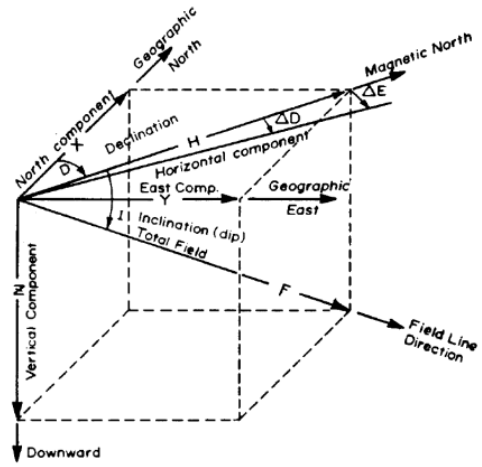

Figure 8.1 – Components of the geomagnetic field for a simple geomagnetic total field F, inclined into the Earth [Campbell, 2003]

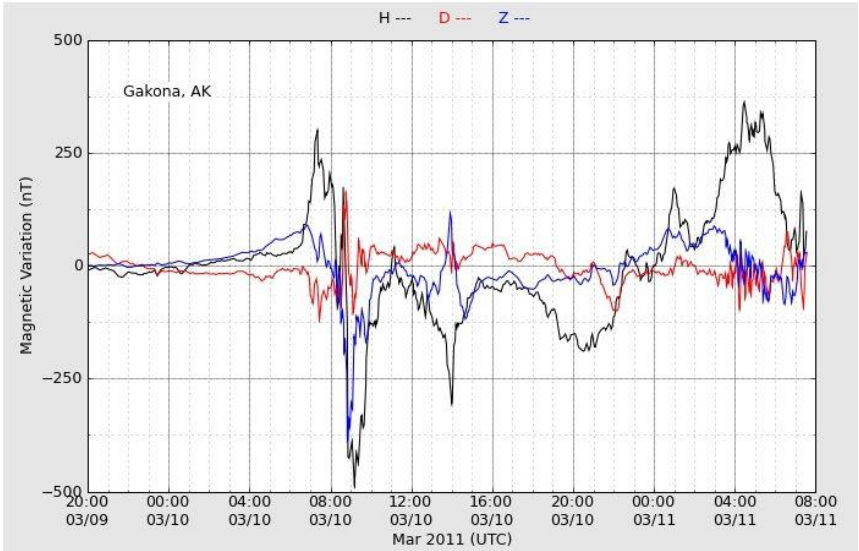

Figure 8.2 – Sample data from a HAARP (High Frequency Active Auroral Research Program) monitored magnetometer at Gakona, AK. H, D, and Z components of the magnetometer are each represented by black, red and blue colors, respectively (http://www.haarp.alaska.edu/cgi-bin/magnetometer/gak-mag.cgi)

In the above plot, there is a minimal geomagnetic activity for the first 8 hours, but afterwards this auroral station begins to see a greater geomagnetic activity, which could be due to the enhancement in auroral currents.

More specifically, we would anticipate seeing a sharp switch in the orientation of the IMF B_Z from +ve to –ve, or Northward to Southward, to indicate the time of magnetic reconnection.
The following figure from a recent paper shows that if this was an IMF B_Z plot, then a reconnection would have occurred around 9 UT.

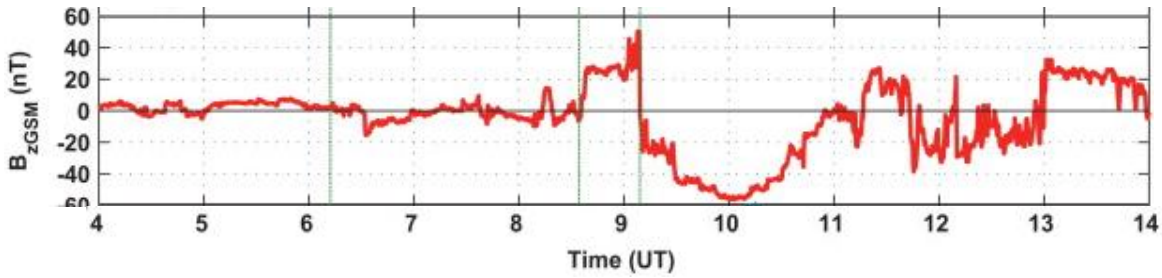

Figure 8.3 - IMF B_Z plot for active sun conditions and the time of magnetic reconnection (shown here at 9 UT) [Sharma, 2012]

Data Transmission

We will use the Universal Space Network (USN) worldwide network of ground stations (PrioraNet: http://www.sscspace.com/ground-network-prioranet-1) for tracking, telemetry and navigation coverage. PrioraNet provides continuous S-band coverage for spacecraft commanding and healthy telemetry. The network's polar sites located at Kiruna, Sweden, and Poker Flats, AK, will cover satellite's transmission for most of the near-apogee section of the orbit. While at perigee, four other sites in Southern hemisphere will be used for transmission, particularly, in Chile, South Africa, Australia, and Antarcatica. An average of hour long coverage per orbit would be sufficient for the downlink of X-band science and other sensors' data.

9. Space Environment Effects

Near Earth space environment is really harsh and projects such deleterious effects that would be unheard of for aircrafts flying in the troposphere. These effects can be divided into multiple distinct categories and explained individually. The spacecraft design team should design around all of these challenges for successful mission operation:

1. Neutral Atmosphere and Launch Effects
    a. Vibrational Effects
    b. Atmospheric Drag
    c. Corrosion Effects
2. Plasma Environment Effects
    a. Communication Disruption
    b. Spacecraft Surface Charging
    c. Deep/ Internal Charging
3. Radiation Environment Effects
    a. Ionization Damage; Ionization Dosage Increase
    b. Single Event Effects (SEEs)
        - SEUs, SELs, SEBs, SETs, SESs, etc.
4. Meteoroidal Environment Effects
    a. Impact-related Mechanical Damage
    b. E&M Radiation Effects
5. Other Space Environment Effects
    a. Harsh Thermal Environment
    b. Orbital Decay due to Oblateness, Magnetic Friction etc.

1. Neutral Atmosphere and Launch Effects:

The neutral molecules pose numerous challenges to the launch vehicle as it tries to escape the Earth's gravitation and its atmosphere.

Vibrational Effects:

First, the spacecraft has to survive the launch-induced vibrations. Thus, the sensitive instruments must be mounted on rubber anti-vibration mounts, and must have proper vibration absorption padding throughout the payload [Ellwood, 1995]. We need the satellite to be able to withstand similar strong vibrations on orbit as well when it passes through the bow shock region on the dayside magnetosphere boundary. This region would, for a very brief time, inflict a strong vibrational shock on the spacecraft.

Atmospheric Drag:

Neutral molecules impose significant resistive force to the launch vehicle, called atmospheric drag, as it passes through the Earth's atmosphere and the Low Earth Orbit. This drag can cause the satellite to lose altitude and hence affect their orbital dynamics, so that the velocity can be regained. Mostly satellites with perigee less than 1000 km are most severely affected by this drag force. Our satellite's radius of perigee would be $2R_E$, which is a high enough altitude for the neutral density to be very low, and the effect of the atmospheric drag to be negligible. So

although our on-orbit satellite would not experience a significant drag, our launch vehicle will experience it as it cruises through the neutral atmosphere.

Moreover, since we will be launching the spacecraft near the solar maximum, we might expect a higher than usual atmospheric drag experienced by the spacecraft. This is because the solar activity heats up the atmosphere and expands it, such that the neutral density increases at higher altitudes. Increased geomagnetic activity also causes increased auroral atmospheric heating due to enhanced electrojets and the resulting neutral wind speeds can exceed 2km/s, increasing the total drag on the spacecraft. Thus, to minimize the atmospheric drag on the launch vehicle we should take into account the F10.7 cm index data that indicates the amount of solar flux and launch the vehicle in low solar flux conditions. Our satellite would also be designed so as to minimize the effective cross-section.

Corrosion:

Also noteworthy are the corrosive effects of the atomic oxygen in the lower earth orbit on several materials, especially silver and other transition metals. Metal oxide layers are formed and continue to break as the thermal stress on the spacecraft is increased. This effect is most severe over the altitudes between 200 and 700km, and would affect our launch vehicle, although our on orbit satellite, beyond $2R_{E,}$ will largely be immune to such problems. Materials such as carbon, silver and osmium are most affected by oxidation and should not be used on external surfaces [Rooij, ESA].

2. Plasma Environment Effects:

Communication Disruption:

Solar radio bursts cause RF waves to be emitted from the sun's surface which can interfere with and disrupt satellite to ground communication and can even result in loss of satellite tracking. Our distant orbit, deep in the magnetosphere, would be more susceptible to this interference because of greater exposure to the solar wind. This can be avoided by scheduling our communications around scintillations. Another intelligent way, adapted by ACE mission, could have been to specifically design the solar exclusive zone orbit so as to naturally avoid solar radio interference [Christian, 2012].

Spacecraft Charging:

Spacecraft charging in the space plasma environment has perhaps accounted for the most mission failures and spacecraft anomalies since the early 1970s when the knowledge of this effect began to become clearer. This can be divided into two categories, namely surface/ differential dielectric charging and the internal/ bulk or deep charging.

1. Surface charging, is driven by the flow of charged plasma particles past the spacecraft body and is largely attributed to the electrons in fewer than 50 keV energy range [DeForest, 1972]; electrons more energetic than these can penetrate the surface to cause internal charging. Moreover, photoelectric effects due to incident sunlight also contribute to this effect, and thus the midnight to dawn sector is most favorable to this phenomenon.

While in eclipse, spacecraft can get charged -ve to tens of kilovolts and becomes ripe for discharge as it emerges into the sunlight, because one side of the spacecraft becomes suddenly positive due to photoelectric emission. Following figure from [Holbert, 2007] shows this effect:

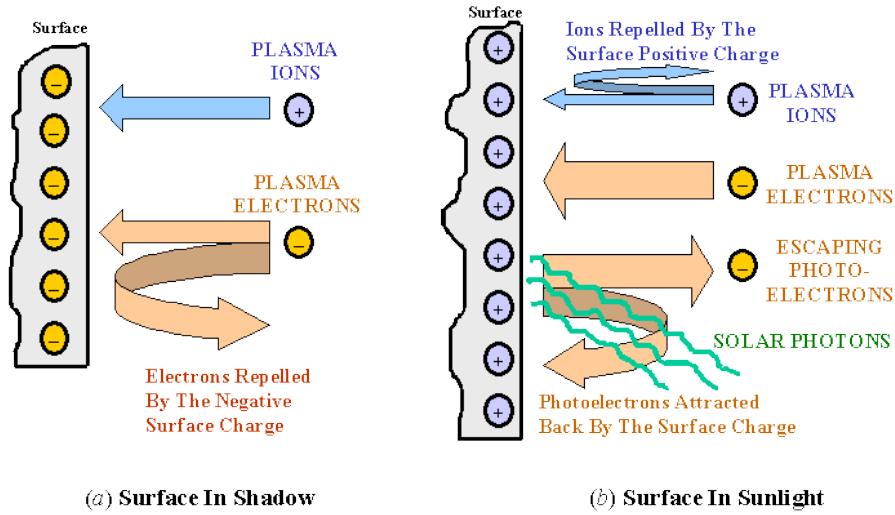

(a) **Surface In Shadow** (b) **Surface In Sunlight**

Similar effect can be observed when a portion of a satellite is under its own shadow as shown below. The side exposed to the sunlight would become positive due to photoelectric emission, while the shadowed side has an increased incident electron flux, because electrons have higher mobility, and will be charged negatively. This is known as differential discharging and is caused due to dielectric portions of the surface, as the charge cannot be quickly redistributed.

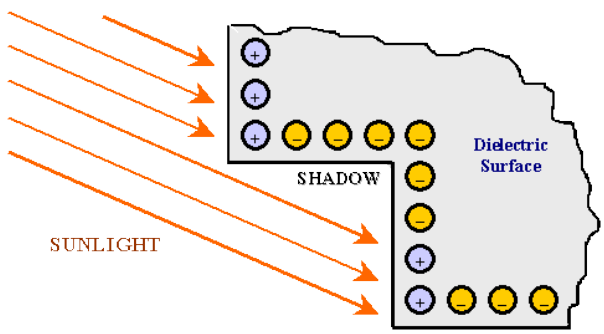

Discharge effects from differential charging can be detrimental causing arc discharges and physical damages. Extreme surface potential differences can go up to 20kV in nightside magnetosphere during eclipse or shadowing, up to 100V in dayside magnetosphere, and up to 200V in dayside magnetosheath [Grard, 1983].

The best way to reduce the surface potentials when non-conducting surfaces (solar panels) are used is to coat the surface with conductive material, e.g. Indium Oxide [Melvin, 1992]. Also to design the spacecraft so that there is a common ground passing through all the internal and surface structures of the spacecraft.

2. Internal Charging is like Single Event Effects (SEEs) that results when particles energetic than 50 keV penetrate the surface and cause large static charging on the electronics. Deleterious discharging can follow and should be avoided by grounding and shielding.

3. Radiation Environment Effects:

Various Space Radiation Environments and their Effects on Micro-electronics		
Radiation Source	**Particle Types**	**Primary Effects in Devices**
Van Allen radiation belts (Trapped Energetic Particles)	Electrons (up to 10MeV)	Ionization damage (TID)
	Protons (up to 100s MeV)	Ionization damage (TID); SEE in sensitive devices
Galactic cosmic rays	High-energy charged particles	Single-event effects (SEEs)
Solar flares	Electrons	Ionization damage (TID)
	Protons (several GeV)	Ionization damage (TID); SEE in sensitive devices
	Lower energy/heavy-charged particles	SEE

Table 9.1 – Various Sources of Space Radiation and their Effects [Wall, NASA ASIC]

Space radiation environment is really hostile to microelectronics and communication systems. Effects of radiation can be categorized into **two notable effects** in devices, namely Total Ionization Dosage (TIDs) and Single Event Effects (SEEs). Both the TIDs and SEEs are caused by different mechanisms. Basically, ionization damages resulting in an increase in TIDs, are caused by both electrons and protons, while only the high energetic particles, especially the heavy protons are responsible for causing the SEEs.

These effects manifest as both analog and digital damages. Electronic noise or signal spikes may be generated as electrons are kicked off through impact ionization of charged particles or cosmic rays. Ionization effects are mostly evanescent, causing glitches and soft errors leading to latchups. All sorts of transistors can be affected by TIDs. BJT gain may reduce through neutron effects, MOSFET performance might decrease with increased hole accumulation in oxides and so on [Holmes-Siedl, 2002]. Overall, satellite lifetime will shorten because of TIDs.

In the digital regime, we see Single Event Latchup (SELs), Single Event Upsets (SEUs) when ions interact with the chip, causing bit flip upsets, Single Event Transient (SETs) causing an electrostatic discharge, Single Event Snapbacks (SESs) causing avalanche multiplication of charge carriers in MOS transistors, and Single Event induced Burnouts (SEBs) causing drain-source voltage to exceed the MOSFETs breakdown voltages etc. SEUs are more common (20/day) due to outgassing when satellite is first put on orbit, but gradually they drop down to 1-2/day.

TIDs and SEEs are the natural and mostly inevitable consequence of the space environment. Radiation hardening is a method by which we can minimize their impact on the success of our mission. It is a way of designing and testing satellite electronics to enable greater resistance to malfunctions cause by the above mentioned ionizing radiation.

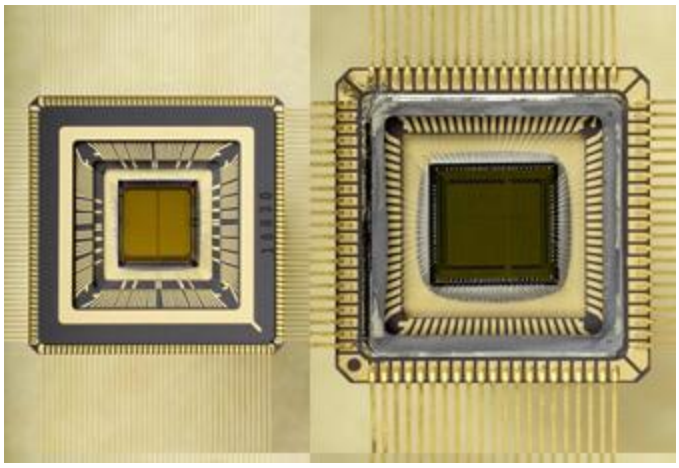

Figure 9.2 – Rad Hard FPGAs by Bae Systems [Ruhl, 2010]

Few of the means by which rad-hard devices are implemented include:

a) Replacing capacitor-based DRAMs with more rugged SRAMs,
b) Making use of additional parity bits for data corruption checks,
c) Designing circuits with more-susceptible CMOS replaced with BJTs whenever possible,
d) Using a wide band gap substrate in transistors that has tolerance to deep-level defects,
e) Employing redundant elements at the system and circuit levels to account for component failures, and
f) Protective coating of polyethylene or hydrogen that provides less secondary ionizing particles, etc.
g) Shielding the chips against radioactivity by e.g. using depleted boron that captures netrons and undergoes alpha decay, etc.

4. Meteoroidal Environment Effects:

Our near Earth space environment has tremendous amount of human-made debris and meteoroids travelling at tens of km/s. While debris is restricted to the LEO orbit, where our satellite will not be stationed, although it will fly past it, meteoroids are found in all orbits, from LEO to GEO and beyond. Many small meteoroids will cause little to no damage to the satellite, but given a large sized heavy meteoroid at LEO, it might cause a significant dent (or even complete penetration) on the satellite's surface. This is because debris in LEO have large speeds relative to other objects than what it has in GEO, e.g. in rare cases, we might even have a penetration into the .25" aluminum body of the satellite, as we saw in the homework problem. Any impact will fragment the meteoroid into pieces which can result in a series of more impacts. Even if significant damage isn't caused by penetration, we might see electrical anomalies due to electromagnetic radiation. Figure below shows how the solar started to tear in two places when redeployed at new location of the International Space Station by the STS-120 mission crew. The cutaway piece of the tear brought to Earth by astronauts and analyzed by NASA showed that the tear was due to characteristic fusing caused by orbital debris and/or meteoroid.

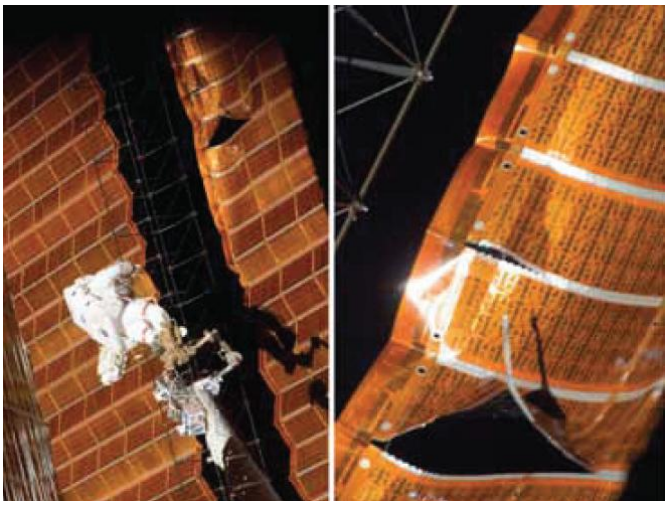

Figure 9.3 – Two tears approximately 30 cm and 90 cm long in the P6 solar array wing 4B after an attempt to redeploy the array during the STS-120 mission [NRC, NASA Debris]

Hence, a whipple shield must be used on the spacecraft to shield the payload and solar panels from catastrophic mechanical damages. Moreover, sensitive instruments like the fuel tank should be installed in protected areas.

5. Thermal and Orbital Decay Effects:

Harsh Thermal Environment

In-orbit satellites work in an environment varying between cold deep space and hot sunlight. Our satellite would see periods of hot sunlight to long cold eclipses with a minimum of heater power provided by the spacecraft. This would present severe challenges for all protruding sensors including our magnetometer boom. These sensors need to be kept at room temperature when operational, and not colder than freezing point when non-operational. This requires special coatings and thermal blanket interfaces on the protruding instruments.

Orbital Decay

Satellite's orbit can decay for many reasons. One of them is the work done against the Earth's magnetic field, which is used to orient the spacecraft. This momentum loss slows down the reaction wheels and results in a loss of attitude control, and hence the orbital decay over time. Our highly elliptical orbit can also be affected by this phenomenon during periods of high geomagnetic activity. This would also cause excessive fuel depletion in station keeping and loss of orientation knowledge. We would implement attitude control with reduced number of gyroscopes and allow for safe mode operations, like tracking the sun, to ensure power generation.

Orbital perturbations can also arise in the highly inclined orbits, where satellites are caused to precess due to the oblateness of the Earth, i.e. Earth is somewhat flattened at the poles ["Army Space Reference Text"].

10. Conclusion

Thus, our satellite will meet its objective of acquiring in-situ the interplanetary magnetic field data at the point of reconnection in the magnetosphere for the 2 year duration of the scientific mission. Thus we will have a good measure of solar wind magnetic field following the various events of geomagnetic storms. In conjunction with the data from other instruments, our magnetometer data will enable us to answer critical scientific questions like, how is magnetic flux transfer following the reconnection dependent on IMF B_Z and other solar wind parameters. Moreover, our spacecraft will be resilient to many known adverse space environment effects and will be able to more strongly endure the harsh radiation, plasma, and meteoroid filled outer space of the Earth.

11. References

["Army Space Ref."] "Space Environment and Orbital Mechanics." *Army Space Reference Text*. US Army Space Institute, n.d. Web. 15 June 2012. <http://www.fas.org/spp/military/docops/army/ref_text/chap5im.htm>

[Bhavnan, 1991] Bhavnani, K. H., and R. P. Vancour. "Coordinate Systems for Space and Geophysical Applications." DTIC *Online*. Phillips Laboratory, Air force Systems Command , 11 Dec 1991. Web. 15 Jun 2012. <http://www.dtic.mil/cgi-bin/GetTRDoc?Location=U2&doc=GetTRDoc.pdf&AD=ADA247550>.

[Campbell, 2003] Campbell, Wallace. Introduction to Geomagnetic Fields. 2nd. Cambridge, UK: Cambridge University Press, 2003. Print.

[Christian, 2012] Christian, Eric, and Andrew Davis. "Advanced Composition Explorer (ACE) Mission Overview." Advanced Composition *Explorer (ACE)*. ACE Science Center, 27 Jan 2012. Web. 15 Jun 2012. <http://www.srl.caltech.edu/ace/ace_mission.html>.

[DeForest, 1972] DeForest, S.E. "Spacecraft charging at synchronous orbit," *Journal of Geophysical Research*, vol. 77, no. 4, pp. 651-659, Feb. 1972.

[Ellwood, 1995] Ellwood, J., B. Gramkow, M. Schwetterle, and R. Schmidt. European Space Agency. *Cluster Payload - A Unique Engineering Challenge*. ESA-European Space Research Institute, 1995. Web. <http://www.esa.int/esapub/bulletin/bullet84/ellw84.htm>.

[Grard, 1983] Grard, R., K. Knott, Pedersen, "Spacecraft charging effects," *Space Science Reviews*, vol. 34, pp. 289-304, 1983.

[Goldstein] Goldstein, Jerry. "Science Implementation." *Magnetospheric Activation and Geospace Ion Circulation Proposal to NASA*. n.d. n. page. Print.

[Holbert, 2007] Holbert, Keith. "Space Radiation Environmental Effects." EEE 598 - Radiation Effects. Arizona State University - Electrical Engineering, 13 Feb 2007. Web. 15 Jun 2012. <http://holbert.faculty.asu.edu/eee560/spacerad.html>.

[Holmes-Siedl, 2002] Holmes-Siedle, A. G., and L Adams. *Handbook of Radiation Effects*. 2nd. England: Oxford University Press, 2002. 643. Print.

[Johnson, 1992] Johnson, M. H., and John Kierein. "Combined release and radiation effects satellite (CRRES) - Spacecraft and mission." *Journal of Spacecraft and Rockets*. 29.4 (1992): 556-63. Web. <http://adsabs.harvard.edu/abs/1992JSpRo..29..556J>.

[Kivelson, 1995] Kivelson, Margaret., and Russell, Christopher, Introduction to Space Physics, Cambridge University Press, 1995

[Wikipedia contributors] Wikipedia contributors. "Radiation hardening." *Wikipedia, The Free Encyclopedia*. Wikipedia, The Free Encyclopedia, 30 May 2012. Web. 15 Jun 2012. <http://en.wikipedia.org/wiki/Radiation_hardening>.

[Melvin, 1992] Melvin, Michael. Thesis: Design and Evaluation of Ion Source for Satellite Charge Control. Monterey, CA: Naval Postgraduate School, 1992. Web. <http://www.dtic.mil/dtic/tr/fulltext/u2/a255172.pdf>.

[NASA GSFC, 2010] NASA Goddard Space Flight Center. *Magnetometry 101: Fluxgate Magnetometers*. 2010. Video. Goddard Multimedia, Greenbelt, MD.

Web. 15 Jun 2012. <http://svs.gsfc.nasa.gov/vis/a010000/a010600/a010682/>.

[NRC, NASA Debris] National Research Council, Committee for the Assessment of NASA's Orbital Debris Programs. "BOX 10.1 Damage Analysis." *Limiting Future Collision Risk to Spacecraft: An Assessment of NASA's Meteoroid and Orbital Debris Programs*. . 1st. Washington, D.C.: The National Academies Press, 2011. 73. Web. 15 Jun. 2012. <http://www.nap.edu/catalog.php?

[PRISM] *PRISM (Picosatellite for Remote-sensing and Innovative Space Missions)*. N.d. Graphic. EO Portal. Web. 15 Jun 2012. <http://www.eoportal.org/directory/pres_PRISMPicosatelliteforRemotesensingandInnovativeSpaceMissions.html>.

[Rooij, ESA] Rooij, A. European Space Agency. *Corrosion in Space*. Noordwijk: European Space Technology and Research Centre, Web. <http://esmat.esa.int/Publications/Published_papers/Corrosion_in_Space.pdf>.

[Ruhl, 2010] Ruhl, Kai. "An introduction to Space Weather." Land of Kain: Space Weather. N.p., 03 2010. Web. 15 Jun 2012. <http://www.land-of-kain.de/docs/spaceweather/>.

[Santo et al, 2001] Santo, Andrew, Robert Gold, et al. "The MESSENGER mission to Mercury: Spacecraft and Mission design." *Planetary and Space Science*. 49.14-15 (2001): 1481-1500. Print.

[Sharma, 2012] Sharma, Shweta, P. Galav, et al. "Study of ionospheric TEC during space weather event of 24 August 2005 at two different longitudes." *Journal of Atmospheric and Solar-Terrestrial Physics*, Vol. 75–76, February 2012, Pages 133-140 <http://www.sciencedirect.com/science/article/pii/S1364682611001441>

[Strangeway, 2001] Strangeway, Robert. "Design." *Fluxgate Magnetometer for NASA/GSFC ST5 Mission*. Institute of Geophysics and Planetary Physics, University of California, Los Angeles, 11 Jun 2001. Web. 15 Jun 2012. <http://www-ssc.igpp.ucla.edu/st5/history.html>.

[Strangeway, 2001] Strangeway, Robert. "History." *Fluxgate Magnetometer for NASA/GSFC ST5 Mission*. Institute of Geophysics and Planetary Physics, University of California, Los Angeles, 11 Jun 2001. Web. 15 Jun 2012. <http://www-ssc.igpp.ucla.edu/st5/history.html>.

[Wall, NASA ASIC] Wall, James, and Anne Macdonald. United States. National Aeronautics and Space Administration. *NASA ASIC Guide: Assuring ASICS for Space*. Pasadena: Jet Propulsion Laboratory, California Institute of Technology, 1993. Web. <http://parts.jpl.nasa.gov/asic/title.page.html>.

[William, 2011] William, Tracy. "Orbital Elements." *NASA: Human Space Flight*. National Aeronautics and Space Administration, 21 Oct 2011. Web. 15 Jun 2012. <http://spaceflight.nasa.gov/realdata/elements/>